ASSOCIAZIONE NAZIONALE ITALIANA DI INGEGNERIA SISMICA ANIDIS
Italian National Association of Earthquake Engineering

XVIII CONVEGNO ANIDIS
L'ingegneria sismica in Italia
ASCOLI PICENO 2019
15-19 Settembre

Experimental and numerical assessment of masonry walls with new openings strengthened with steel frames

Mónica Y. Oña Vera[a], Giovanni Metelli[a], Joaquim A. O. Barros[b], Giovanni Pizzari[a]
[a] *Dipartimento di Ingegneria Civile, Architettura, Territorio, Ambiente e di Matematica, Via Branze 43, 25123 Brescia.*
[b] *ISISE, IB-S, Department of Civil Engineering, University of Minho, Campus de Azurém, 4800-058, Guimarães, Portugal.*

Keywords: Steel frame; Dry-driven dowels; Unreinforced masonry brick walls; new openings.

ABSTRACT
The creation of new openings in masonry walls is a frequent intervention executed in existing buildings. Depending on their size and position, these interventions may cause significant decrease of the wall's original in-plane strength and stiffness, thus compromising the building seismic resistance. In masonry buildings, strengthening techniques aim to restore as much as possible the loss of stiffness and strength, be reversible and respect the compatibility between materials, particularly in the case of historical buildings. In an attempt to complying with these requirements, engineering practitioner often introduce very stiff steel profiles forming a frame inside the opening for fully restoring the stiffness and resistance without substantially increasing the building's own weight. Moreover, they can guarantee an adequate level of reversibility. However, the effectiveness of this technique is typically quantified using linear elastic analysis and a simple sum of the flexural and shear stiffness of the masonry panels and the steel frame. The present work aims to improve the knowledge and better quantify the effectiveness of this traditional steel frame technique, through experimental and numerical methods. The experimental program was designed to provide full assessment of the effects of introducing a new door opening in brick masonry walls, from the perforation process to the application of in-plane cyclic loads. The steel frame was designed using numerical tools and consisted in four profiles welded together and tied to the surrounding masonry wall by means of dry-driven dowels. Results show that the steel frame system restores the original solid wall's in-plane strength and ductility, but not the lateral stiffness.

1 INTRODUCTION

The highest earthquake hazard is concentrated in south-eastern areas of Europe, which include most of the Italian territory where clay masonry buildings prevail. The majority of such structures were built before the release of seismic codes, when the living demands were different from the current decade. Nowadays, many of these structures are modified to satisfy present owners requests. Such modifications often include the creation of new openings for windows, doors or simply ducts for heating, ventilation, and air conditioning. Typically, small openings would hardly affect the structural behaviour of masonry shear walls or buildings. The problem emerges when these openings increase in number or size and are located in a critical position (e.g., when several garages are created at the street level; Figure 1a), thus increasing the vulnerability of the structure. In particular, there is an increase of the risk of a soft-storey mechanism of collapse during an earthquake. Another problem emerges when a door of significant size is introduced in a continuous shear masonry wall, reducing the cross section of the remaining piers and spandrel and, thus, weakening the wall's in-plane stiffness and strength. These changes in the original wall seismic strength, have consequences in the remaining shear walls, e.g., larger earthquake load demands than their shear capacity. The latter problem was studied by Ona and co-workers (Ona 2018a), through numerical modelling for evaluating the effects of opening sizes and positions in the wall's in-plane response. The Authors found that the opening position defines the dominant collapse mechanism and that the decrease in percentage of shear Strength (V) and stiffness (K), when creating an opening, is proportional to the opening size (Ona et al., 2018b).

According to the Italian Structural Code (NTC 2018), *new openings should be avoided to the utmost; and when this is not possible, the remaining wall must be reinforced, such that the stiffness, strength and mass do not change substantially and that the new opening does not lead to a reduction of pre-existing levels of safety, by compromising a proper distribution of lateral forces.* The International Scientific Committee for

Analysis and Restoration of Structures of Architectural Heritage Guidelines (ICOMOS 2003) requires that, when working with masonry structures, compatibility of materials, reversibility and aesthetics of the architecture must be considered. To satisfy these requirements and the requirements of (NTC 2018), engineering practitioners often use a steel frame surrounding the opening and connected to the masonry by means of steel bars or welded shaped plates; this system seems reversible as, if necessary, it can be easily removed. The components of this frame are either i) small steel profiles, designed for vertical loads only and typically found in openings realized before the introduction of the seismic requirements or ii) very stiff profiles, in an attempt of fully restoring the loss of in-plane stiffness and strength (Figure 1b).

a) b)

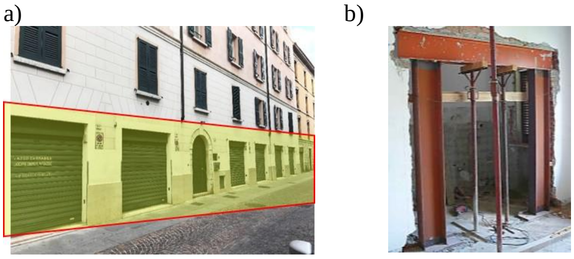

Figure 1 a) New openings at the street-level of an unreinforced masonry building in Brescia (Italy); b) Steel frames in new garage (font: www.ingegneriapresenti.it).

To the date, the design of the steel frame technique is based in the Timoshenko beam theory and linear elastic analysis (Pugi 2010), in line with the Italian guidelines (C.M. 2019) and the interpretative guidelines proposed by the Technical Scientific Committee for the local intervention or strengthening of existing buildings is seismic areas (CTS 2010). These calculations consider the elastic stiffness as a function of the masonry panel gross section, thus the spandrel contribution is neglected in the case of a wall with new openings. As observed by (Parisi 2014), spandrels may increase the wall shear capacity depending on their geometry, interlocking effects and the presence of lintel or tying elements. Thus, it is expected that typical calculations overestimate the walls' loss of stiffness due to new openings. In fact, Ona 2018a, Billi et al. 2019 observed that these calculations predict a loss of stiffness equal to 75% of the original solid wall stiffness, when a new opening (representing 20% of the wall's total area) is executed in a masonry wall assumed as a cantilever beam. Where double fixed boundary conditions are possible, the loss of stiffness is equal to 55%. Such predictions have consequences in the design of the steel frame, as very large or stiff steel profiles are required to restore the original stiffness of the solid wall (Pugi 2010, Ona 2018a, Billi 2019). Another drawback of the current guidelines and typical calculations is the definition of stiffness, which is the secant stiffness (according to NTC 2008) and defined as 50% of the elastic stiffness (calculated as the sum of the flexural and shear stiffness of the masonry panels). However, in this calculation, the Young Modulus of masonry has the same value before and after the new opening. In practice, this assumption might not be adequate, as the perforation process and the brittle nature of masonry can easily develop several small or large cracks, which can affect this material property (Ona 2018a).

Due to the lack of experimental data, it is then, almost impossible, to quantify the real loss of stiffness and strength due to new openings; and the effectiveness of the steel frame strengthening technique to restore both. The present paper shows the results of a large research work (Ona 2018a) aimed to contribute to this lack of knowledge. Therein, a clay masonry wall was built as solid, perforated to create a new door opening, and strengthen with a steel frame connected to the surrounding masonry by means of steel dowels welded to the frame and dry-driven in the bricks. The wall was afterwards tested under quasi static cyclic in-plane loads under displacement control. Several numerical analysis were also carried out, first for the design of the wall specimen with steel frame and, then, to evaluate the specimen performance against a solid wall and a unreinforced wall with opening. The results of these numerical calculations are summarized herein.

2 EXPERIMENTAL PROGRAM

2.1 *Wall specimen and strengthening steel frame*

The wall specimen is made of clay brick of average dimensions of 245 mm x 120 mm x 60 mm stacked together with the Flemish bond pattern and 10 mm thick bed-joints filled with weak mortar (f_c=5 MPa). The specimen was originally built as a solid wall of 3140 mm x 1980 mm and then perforated using a diamond grinding disk (Figure 2a) to create a new door opening of 1010 mm x 1550 mm. The steel frame consisted in four profiles type HEA140, welded together to form a closed-ring shape, fixed to the masonry wall by means of smooth steel dowels (S355) of 16 mm diameter, dry-driven in the bricks' header or stretcher centre of geometry. The dowels were positioned according to a staggered framework avoid weakening the surrounding masonry (see section A-A' in Fig. 3). The spacing between dowels was ~210 mm. Finally, the opposite head of the dowels was welded to the steel profiles' flanges to ensure fixed ends and exploit the dowels' maximum shear stiffness. To close the gap between the steel profile and masonry wall and to distribute the axial pressure from masonry to frame, a layer of 30 mm of strong mortar was poured (Figure 2b). The wall specimen positioned in the experimental set-up is shown in Figure 2c. The dowels total length was 200 mm, while the embedded length inside the brick, mortar and steel flange was 150 mm. The choices of the dowels length and welded heads were based on the estimation of the dowel capacity proposed by (Giuriani 2012).

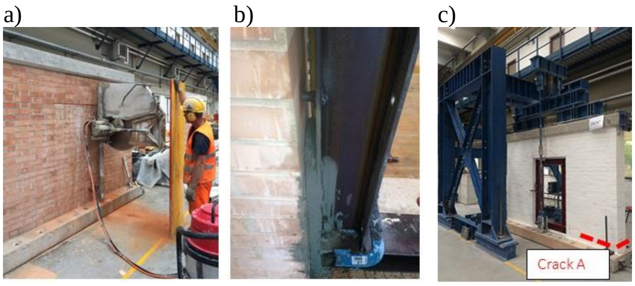

Figure 2 a) Perforation process; b) detailing of the technique; c) wall specimen before the in-plane test.

2.2 *Experimental setup*

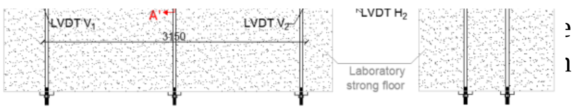

Figure 3. The vertical load acting on the wall was equal to 250 kN (σ_V=0.32 MPa). It was calculated for a two-storey house and represents 5.5% of the masonry compressive strength. The vertical load was applied to the wall using a hydraulic jack which distributed the pressure through a series of steel beams that were in contact with a Reinforced Concrete (RC) beam lying on 20 mm of strong mortar layer (f_c=20MPa at 28 days), in contact with the masonry wall. The vertical jack was self-balanced with a beam rigidly anchored to the laboratory strong floor. The horizontal force was applied in displacement control and in both sides of the top RC beam, using two steel plates connected to the jack by a steel bar running through the beam mid-section. The force was applied using a 500 kN capacity electro-mechanic actuator that reacted against a steel braced frame (Figure 3). As schematized in Figure 3, when the steel loading plate 1 pushed the loading cell towards the right direction, the load was assumed as positive, whereas the opposite (pulling, using plate 2) was assumed negative.

Several Linear Variable Differential Transformers (LVDT) were used to monitor the lateral displacements of the wall with reference to the laboratory strong floor; possible slippage between the concrete foundation and the laboratory strong floor; and any rotations of the concrete base. Further details can be found in (Ona 2018a).

The test was divided in two phases because of a bed-joint crack ("Crack A" in Figure 2c) that influenced the wall's in-plane hysteresis response during the first part of the test (Phase 1). This crack was developed before the cutting-out process, when the Dywidag bars passing through the RC base were fixed to the strong floor of the laboratory. This action caused small deflections of the RC beam, which led to the formation of two bed-joint cracks at the base and mid-height of the right pier, being the most relevant Crack "A". This crack was afterwards repaired, using a grouting mortar and the test was re-started (Phase 2). Yet, during Phase (1) the wall suffered some damaging and other bed-joint crack developed in the opposite pier. The test was stop when the wall shear capacity dropped by 20 %. The loading history and aforementioned test setup are in line with previous in-plane tests carried out by the same research group, further details are found in (Ona et al. 2018b).

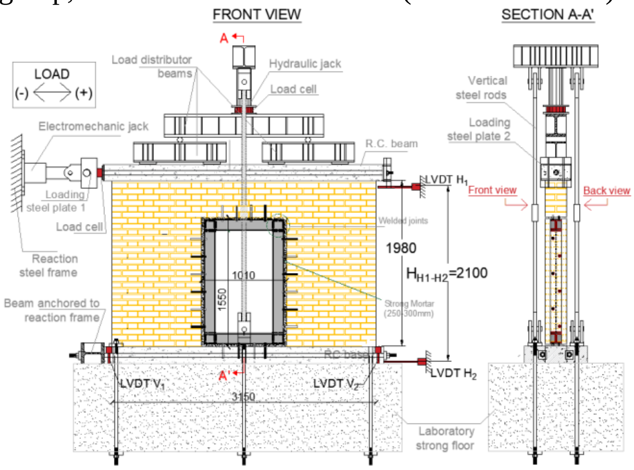

Figure 3 Set-up used for the in-plane test.

3 NUMERICAL MODEL

The numerical simulations were carried out in two phases: (1) prior to the in-plane test to design the steel frame reinforcement (Ona 2018a); (2) after the experimental test to validate the analysis carried out in Stage (1). Herein, only Stage (2) is presented. The numerical macro-models use the smeared approach which is based in the Total Strain Fixed Crack Model available in the Finite Element program Diana FEA (2017). The fixed crack concept was chosen over the rotating because of its permanent memory of damage orientation, which is more compatible with the physical meaning of cracking as the orientation of cracks does not change during the analysis.

The mesh is shown in Figure 4a, where the masonry material was modelled with quadrilateral isoparametric 4-node plane stress finite elements with 2x2 integration points, solved with the Gauss-Legendre method. The steel profiles were modelled with 2-node Bernoulli beam type elements with 6 degrees of freedom. The steel dowels were modelled using 2-node spring elements (1 node belonged to the steel frame and the opposite node to the masonry wall). Finally, the axial forces acting perpendicular to the steel profile (induced by the contact between the masonry and the frame) were simulated using 2-node no-tension springs.

The masonry inelastic deformation in compression followed a parabolic stress-strain relationship, while the tension-softening law was the curve proposed by (Hordjik 1991), dependent on the fracture energy and crack bandwidth (equal to the square root of the element area). The post-cracked shear stiffness was simulated using a damage function. The values used for the constitutive laws are listed in Table 1. Two simulations were carried out, each using the two values of the Young modulus available: E_y=10585 MPa (in the direction perpendicular to the mortar bed-joints) and E_x=5344 MPa (parallel to the bed-joints), both gathered from wallets tested according to European standards (Ona 2018a). The tensile strength (f_t) was calculated as in Eq. (1) (Rots 1997), while the compressive fracture energy (G_c) was calculated as in Eq. (2) (Lourenço 2009), multiplied by a reduction factor of 0.5, to account for a conservative value, as this equation was originally proposed for plain concrete.

$$f_t = c\,/\,(2\mu) \tag{1}$$

$$G_c = d_u\ f_c \tag{2}$$

where f_t is the tensile strength; c is the cohesion and μ is the friction coefficient, both obtained from standard tests (Ona 2018a), d_u=1.6 according to (CEB-FIP Model Code 90), f_c=compressive strength. The stiffness of the no-tension springs *(k_x)* was calculated considering the mortar stiffness and the steel profile's flanges bending stiffness. The complete calculation and equations are detailed elsewhere (Ona, 2018a). Finally, the shear connectors stiffness *(k_y)*, was simulated using the constitutive law shown in Figure 4b(a)

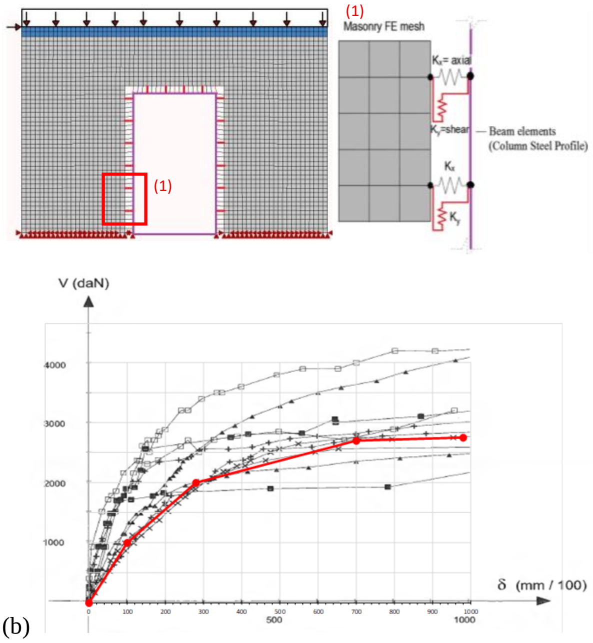

Figure 4 a) Mesh with detailing, where k_x is the stiffness of the no-tension springs and k_y is the stiffness of the springs representing the shear dowels; b) Constitutive law for shear springs (red curve) with results obtained by (Giuriani 2012).

, obtained from experimental shear-slip tests of (Giuriani 2012).

Table 1 Masonry material properties

Young Modulus	E_y =10.6 GPa E_x =5.34 GPa
Compressive strength	6.3 MPa
Tensile strength	0.18 MPa
Compressive Fracture Energy	5 N/mm
Tensile Fracture Energy	0.1 N/mm

(a)

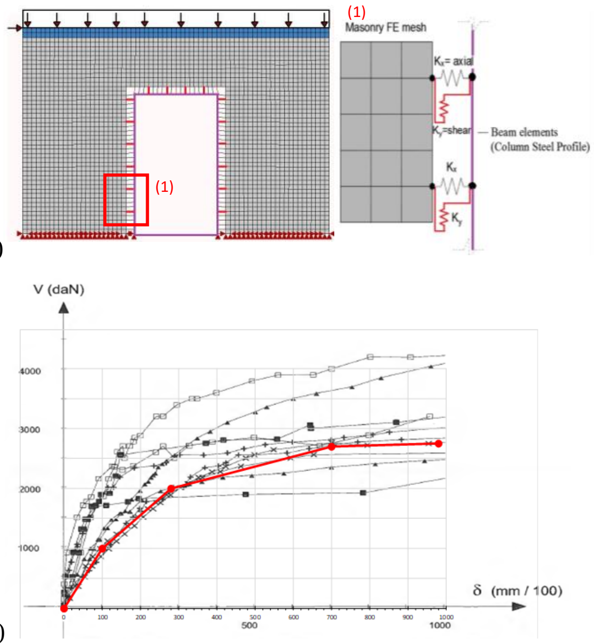

(b)

Figure 4 a) Mesh with detailing, where k_x is the stiffness of the no-tension springs and k_y is the stiffness of the springs representing the shear dowels; b) Constitutive law for shear springs (red curve) with results obtained by (Giuriani 2012).

4 RESULTS

The experimental crack patterns observed after Phase (2) are shown in Figure 5a. As mentioned in Section 2.1, Crack A and B developed prior to Phase (1). By the end of Phase (1) some cracks were noticeable at the spandrel level and at the bed-joint of the left pier (crack C). One may notice the cracks around dowels, which developed as consequence of the rocking behaviour of both piers, i.e., when pushing, the compressive strut is concentrated along one pier, thus, the opposite pier is lifted and the dowels oppose resistance to this lifting. When pulling, a mirrored behaviour occurred. This dowels action guaranteed that the wall behaves as a single panel, i.e., as if no opening would exist. One should notice that the dominant mechanism was rocking behaviour and the numerical cracks which are in agreement with the experimental ones; in particular, it can be observed the cracks surrounding the spring elements working in shear (Figure 5b Figure 5 Experimental and numerical crack patterns). The experimental envelopes from Phase (1) and (2) and the numerical curves using two possible modulus of elasticity E_y and E_x are plotted in Figure 6a, all in the same positive quadrant. It is noticeable the abnormal behaviour of the envelopes (+Load, Phase 1) and (- Load, Phase 2) attributed to the bed-joint cracks "A" and "C". When the wall was pushed towards the direction which closed the crack, the wall exhibited lower stiffness with respect to the opposite direction when the cracks were opened.

It is also notable the potentiality of the numerical model in reproducing with fair accuracy the initial stiffness, and peak strength of the wall in Phase (2), after the cracks were repaired. In particular, the model using the smallest value of the Young Modulus *(E_x)* was more accurate in capturing the stiffness degradation and ultimate displacement. This can be attributed to the masonry damage condition. The wall specimen herein tested presented some damage prior to the test's Phase (1), due to the perforation process, and showed more visible cracks at the spandrel level before starting Phase (2); thus, numerical results are consistent.

a) b)

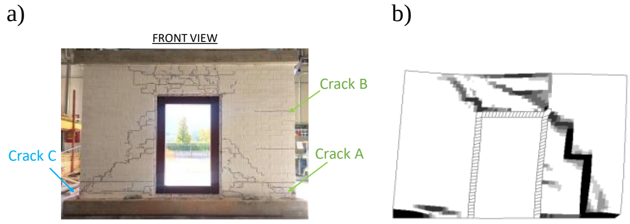

Figure 5 Experimental and numerical crack patterns

5 EFFECTIVENESS OF THE STEEL FRAME

With the numerical model validated by experimental results, further analyses were carried out to evaluate a solid wall (SW), a wall with opening but without reinforcement (PW) and with a very stiff steel frame (with HEA240 beams). The latter frame was obtained from the calculations based in the Timoshenko Beam Theory. Figure 6b shows the results of these simulations and evidences that neither the steel frame type HEA140 nor HEA240 are capable of fully restoring the solid wall's stiffness; and that the profile HEA240 presents a rather brittle response. This is reasonable, as the brittle masonry starts cracking before activating the frame shear stiffness. While the more flexible HEA140 profile is activated earlier and provides a more favourable, ductile response, as also requested by the (NTC 2018 and C.M. 2019).

a)

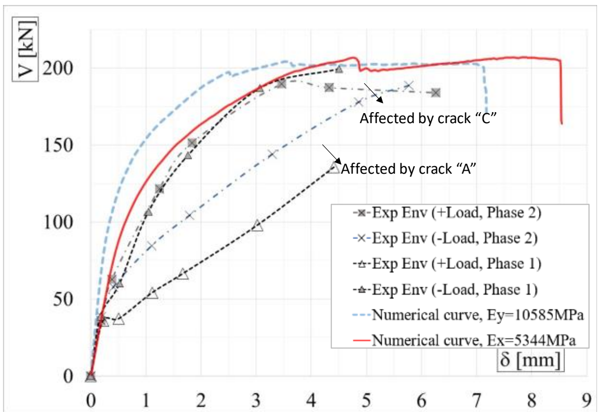

b)

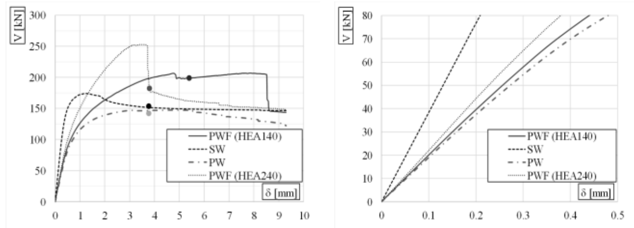

Figure 6 a) Experimental vs. numerical results; b) numerical results

6 CONCLUDING REMARKS

The paper presents a numerical and experimental assessment of the effectiveness of a steel frame reinforcement to restore the loss of in-plane stiffness and strength due to new openings in masonry shear walls. The following outcomes can be drawn: (i) numerical results have proven that very stiff profiles for the steel frame might lead to a brittle response of the wall with opening, as the surrounding masonry starts cracking before activating the frame; (ii) experimental and numerical results have proven the effectiveness of a more flexible profile type in preserving the wall ductility and in-plane strength. However, neither a flexible nor a very stiff profile are capable of restoring more than 60% of the original solid wall's stiffness.

ACKNOWLEDGEMENTS

Financial support for the first author by the Italian Ministry of Education, University, and Research (MIUR) for her Doctoral Scholarship is gratefully acknowledged. The Authors also thank the technicians A. del Barba, A. Botturi from laboratory Pietro Pisa and Eng. J. Rebuzzi, Eng. A. Mangano for their valuable contribution in the experimental activities.

REFERENCES

Billi, L., Laudicina, F., Salvatori, L., Orlando, M. & Spinelli, P. 2018. Forming new steel-framed openings in load-bearing masonry walls: design methods and non-linear finite element simulations, *Bull Earthquake Eng*, **17**(5):2647-2670.

CEB-FIP Model Code-90 London: Thomas Telford Services Ltd., ISBN 978-0-7277-1696-5.

C.M. 2019 Istruzioni per l'applicazione dell'Aggiornamento delle Norme tecniche per le costruzioni di cui al decreto ministeriale 17 gennaio 2018.

CTS 2010 Comitato Tecnico Scientifico in materia di rischio sismico, Orientamenti interpretative in merito a interventi locali o di riparazione in edifici esistenti, (in Italian). D.G.R. No 606 del 21/06/2010.

DIANA FEA 2017. *Diana Finite Element Analysis program*, User's manual. Release 10.2. The Netherlands.

Giuriani, E. 2012. *Consolidamento degli edifici storici* (in Italian). Ed UTET Scienze Tecniche ISBN-13 978-8859807636.

Hordijk, D.A. 1991. *Local approach to fatigue of concrete*. PhD Thesis, Delft University of Technology, Delft University Press, Delft (NL).

ICOMOS 2003. *International Scientific Committee for Analysis and Restoration of Structures of Architectural Heritage Guidelines. Recommendations for the analysis, conservation and structural restoration of architectural heritage*.

Lourenço, P.B. 2009. *Recent advances in masonry structures: micromodelling and homogenization*. In: Galvanetto U, Aliabadi MHF, editors. London: Imperial College Press, pp 6-7.

NTC 2018. Aggiornamento delle Norme tecniche per le costruzioni. Ministero delle Infrastrutture e dei Trasporti, G.U.S.O. n.30 on 17/01/2018.

Ona, M. 2018a. *Local interventions in unreinforced masonry walls: new openings and seismic retrofitting strategies*. PhD Thesis, Università degli Studi di Brescia, Italy.

Ona, M., Metelli, G., Barros, J.A.O., & Plizzari, G. 2018b. Effects of new openings on the in-plane behaviour of unreinforced brick masonry walls. *Proceedings of the 10th International Masonry Conference*, July 9-11. Milan, Italy.

Parisi, F., Augenti, N. & Prota, A. 2014. Implications of the spandrel type on the lateral behavior of unreinforced masonry walls. *Earthquake Eng Struct. Dyn*. 43:1867-1887.

Pugi, F. 2010. *Interventi nelle murature e nuova normativa sismica: Aperture e Cerchiature in Murature portanti con telai in acciaio e in calcestruzzo armato*, Ed. AEDES. ISBN: 978-88-6055-566-3.

Rots, J.G. 1997. *Structural masonry: an experimental/nume rical basis for practical design rules*, Ed. AA Balkema, ISBN 9789054106807.